ABOUT A STRAIN SMOOTHING TECHNIQUE IN FINITE ELEMENT METHOD

Nguyen Xuan Hung [1], Nguyen Dinh Hien [2], Ngo Thanh Phong[1]
(1)University of Natural Sciences, VNU – HCM
(2)University of Technical Education HCMc
(Manuscript Received on April 15th, 2007)

ABSTRACT: *This paper presents a global review of the strain smoothing method to finite element analysis for two-dimension elastostatics. The strain at each point is replaced by a non – local approximation over a smoothing function. With choosing a constant smoothed function and applying the divergence theorem, the stiffness matrix is calculated on boundaries of smoothing elements (smoothing cells) instead of their interior. The presented method gains a high accuracy compared with the standard FEM without increasing computational cost.*

1.INTRODUCTION

In Finite Element Method (FEM), an important work to compute the stiffness matrix is often to use mapped elements, such as the well-known isoparametric elements through Gauss quadrature rule. Then the element stiffness matrix is evaluated inside element instead of along boundaries of element. In using a mapped element, a one – to – one coordinate transformation between the physical and natural coordinates of each element has to be ensured. To satisfy this requirement, the convex element is not broken and a violently distorted mesh is not permitted.

Purpose of this paper is: 1) to construct the element stiffness matrix along its boundaries via a strain smoothing method, 2) to utilize a stabilized method with selective cell-wise strain smoothing when solving nearly incompressible elastic problems, 3) to estimate the reliability of presented method through numerical examples.

2. GOVERNING EQUATIONS AND WEAK FORM

Let $\Omega \subset \Re^2$ be a bounded domain with a polynomial boundary Γ. The body force $\boldsymbol{b}$ is acting within the domain. The governing equilibrium equation for isotropic linear elasticity writes

$$\nabla.\boldsymbol{\sigma} + \boldsymbol{b} = 0 \quad \text{in} \quad \Omega \tag{1}$$

where $\boldsymbol{\sigma}$ is the symmetric Cauchy stress tensor. The compatibility equation is

$$\boldsymbol{\varepsilon} = \nabla_s \boldsymbol{u} = \frac{1}{2}(\nabla \boldsymbol{u} + \nabla^T \boldsymbol{u}) \quad \text{in} \quad \Omega \tag{3}$$

The displacement field satisfies the Dirichlet boundary conditions

$$u_i = \overline{u}_i \text{ on } \Gamma_u \tag{4}$$

and the stress field satisfies the Newman boundary conditions

$$\sigma_{ij} n_j = \overline{t}_i \quad \text{on} \quad \Gamma_t \tag{5}$$

where $\Gamma = \partial\Omega, \Gamma = \Gamma_u \cup \Gamma_t, \Gamma_u \cap \Gamma_t = \varnothing$.

The virtual work equation is of the form

$$\int_\Omega \mu\boldsymbol{\varepsilon} : \boldsymbol{D}_{dev} : \boldsymbol{\varepsilon} d\Omega + \int_\Omega K\boldsymbol{\varepsilon} : (\nabla . \boldsymbol{u1}) d\Omega = \int_\Omega \boldsymbol{b}.\boldsymbol{u} d\Omega + \int_{\Gamma_t} \bar{\boldsymbol{t}}.\boldsymbol{u} d\Gamma \tag{6}$$

The stress field is split into two parts: the deviatoric stress $\boldsymbol{s}$, and the pressure p

$$\boldsymbol{\sigma} = \boldsymbol{s} + p\boldsymbol{1} = \mu\boldsymbol{D}_{dev}\boldsymbol{\varepsilon} + K\nabla.\boldsymbol{u1} \tag{7}$$

where $\boldsymbol{1}$ is the rank two identity tensor, which can be presented by $\boldsymbol{1} = [1 \quad 1 \quad 0]^T$, $\mu\boldsymbol{D}_{dev}$ is the deviatoric projection of the elastic matrix $\boldsymbol{D}$, μ is the shear modulus and K is the bulk modulus defined by $K=E/3(1-2\nu)$, E is Young's modulus, and ν is Poisson's ratio.

Assume that the bounded domain Ω is discretized into n non-overlapping elements, $\Omega \approx \Omega^h = \bigcup_{e=1}^{n_e} \Omega^e$. The standard finite element solution $\boldsymbol{u}^h$ of a finite element displacement model is expressed as follows

$$\boldsymbol{u}^h = \sum_{i=1}^{np} N_i q_i = \boldsymbol{Nq} \tag{8}$$

where np is total number of nodes of mesh, N_i is the shape function of node i, q_i are the associated degrees of freedom at that node. The discrete strain field is

$$\boldsymbol{\varepsilon}^h = \nabla_s \boldsymbol{u}^h = \boldsymbol{Bq} \tag{9}$$

where $\boldsymbol{B} = \nabla_s \boldsymbol{N}$ is the strain – nodal displacement matrix (the discretized, symmetric gradient operator).

By substituting Eq. (8) - (9) into Eq. (6), we obtain a linear system for $\boldsymbol{q}$,

$$\boldsymbol{Kq} = \boldsymbol{g} \tag{10}$$

where the element stiffness matrix given by

$$\boldsymbol{K} = \mu \int_{\Omega^e} \boldsymbol{B}^T \boldsymbol{D}_{dev} \boldsymbol{B} d\Omega + K \int_{\Omega^e} \boldsymbol{B}^T \boldsymbol{D}_\lambda \boldsymbol{B} d\Omega \tag{11}$$

with

$$\boldsymbol{D}_{dev} = \frac{1}{3}\begin{bmatrix} 4 & -2 & 0 \\ -2 & 4 & 0 \\ 0 & 0 & 3 \end{bmatrix}, \quad \boldsymbol{D}_\lambda = \begin{bmatrix} 1 & 1 & 0 \\ 1 & 1 & 0 \\ 0 & 0 & 0 \end{bmatrix} \tag{12}$$

and the load vector is

$$\boldsymbol{g} = \int_{\Omega^e} \boldsymbol{N}^T \boldsymbol{b} d\Omega + \int_{\Gamma_t^e} \boldsymbol{N}^T \bar{\boldsymbol{t}} d\Gamma \tag{13}$$

3. THE STRAIN SMOOTHING METHOD

The strain smoothing method was proposed by Chen *et al.* [1] and Yoo *et al.* [3] as a normalization of the local strain field. This technique is also known as strain smoothing stabilization, through which the nodal strain is computed through the divergence of a spatial average of the standard local strain field. In mesh-free methods [2], this is sufficient to eliminate defective modes through smoothed strains. The derivatives of the shape functions are

not required at the nodes. Applications of strain smoothing to the FEM can be seen as a stabilized conforming nodal integration method as defined in Galerkin mesh-free methods. Strain smoothing at an arbitrary point writes

$$\tilde{\varepsilon}_{ij}^{h}(\mathbf{x}_C) = \int_{\Omega^h} \varepsilon_{ij}^{h}(\mathbf{x})\Phi(\mathbf{x}-\mathbf{x}_C)d\Omega \tag{15}$$

where Φ is a smoothing function. There are several choices for this smoothing function. For simplicity, Φ is assumed to be a step function as follows

$$\Phi(\mathbf{x}-\mathbf{x}_C) = \begin{cases} 1/A_C, \mathbf{x} \in \Omega_C^e \\ 0, \mathbf{x} \notin \Omega_C^e \end{cases} \tag{16}$$

with A_C is the area of the smoothing cell, $\Omega_C^e \subset \Omega^e \subset \Omega^h$, shown in Figure 1.

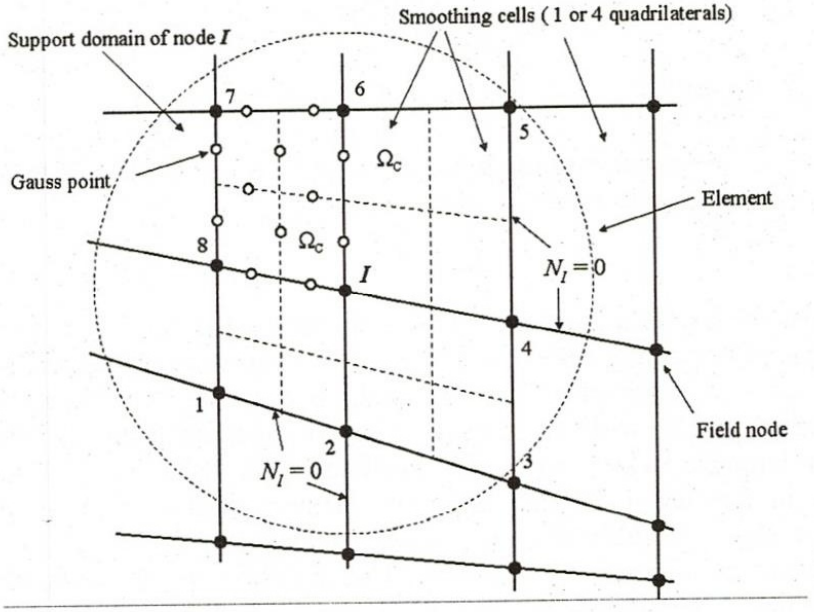

Figure 1: Example of finite element meshes and smoothing cells

Substituting Eq. (16) into Eq. (15), and using the divergence theorem, we obtain

$$\tilde{\varepsilon}_{ij}^{h}(\mathbf{x}_C) = \frac{1}{2A_C}\int_{\Omega_C^e}\left(\frac{\partial u_i^h}{\partial x_j}+\frac{\partial u_j^h}{\partial x_i}\right)d\Omega = \frac{1}{2A_C}\int_{\Gamma_C^e}(u_i^h n_j + u_j^h n_i)d\Gamma \tag{17}$$

Now, consider an arbitrary smoothing cell, $\Omega_C^e \subset \Omega^h$, illustrated in Figure 1 with boundary $\Gamma_C^e = \bigcup_{b=1}^{nb}\Gamma_C^b$, where Γ_C^b are the boundary segments of Ω_C^e, and nb the total number of edges of each smoothing cell. The relationship between the strain field and nodal displacement is corrected by replacing B by $\tilde{B}$:

$$\tilde{\varepsilon}^h = \tilde{\boldsymbol{B}} q \tag{18}$$

The elemental stiffness matrix then writes

$$\tilde{K} = \mu \int_{\Omega^e} \tilde{\boldsymbol{B}}^T \boldsymbol{D}_{dev} \tilde{\boldsymbol{B}} d\Omega + K \int_{\Omega^e} \tilde{\boldsymbol{B}}^T \boldsymbol{D}_{\lambda} \tilde{\boldsymbol{B}} d\Omega \tag{19}$$

Here, the integrands are constant over each Ω_C^e and the non-local strain displacement matrix is in the form

$$\tilde{\boldsymbol{B}}_i(\mathbf{x}_C) = \frac{1}{A_C^e} \int_{\Gamma_C^e} N_i \boldsymbol{n}^T d\Gamma \tag{20}$$

From Eq. (20), we can employ Gauss line integration along each segment, Γ_C^b. If the shape functions are linear along the boundaries of the smoothing cells, one Gauss point is sufficient for exact integration of the weak form. In this case,

$$\tilde{\boldsymbol{B}}_i(\mathbf{x}_C) = \frac{1}{A_C^e} \sum_{b=1}^{nb} N_i(\mathbf{x}_b^G) \boldsymbol{n}^T l_b^C \tag{21}$$

where $\mathbf{x}_b^G$ and l_b^C are the midpoint (Gauss point) and the length of Γ_b^C, respectively.

Considering a mixed variational principle based on an assumed strain field [4], the following system of linear algebraic equations is obtained

$$\tilde{\boldsymbol{K}} q = \boldsymbol{g} \tag{22}$$

In strain smoothing technique, the element is subdivided into *nc* non-overlapping sub-domains also called smoothing cells. For example, the element is partitioned into 1-subcell, 2-subcell, 3-subcell and 4-subcell. Then the strain is smoothed over each sub-cell. While choosing a single subcell yields an element which is superconvergent in the H1 norm, and insensitive to volumetric locking, as shown in Reference [6, 7], if $nc > 1$, locking reappears. It is also shown in Reference [6] that the finite element method with strain smoothing is equivalent to a stress (equilibrium) formulated element for $nc=1$, and tends toward the standard displacement solution for $nc \to +\infty$. Consequently, as *nc* approaches 1, the stress results become more accurate, while the displacement results deteriorate; and as *nc* increases, displacement results gradually improve, while stress results deteriorate.

The purpose of this article is to use a single subcell smoothing to compute the volumetric part of the strain tensor, while the deviatoric strains are written in terms of an arbitrarily high number of smoothing cells. The method may be coined *a stabilized method with selective cell-wise strain smoothing* [8].

The stiffness matrix is built

1. Using $nc > 1$ subcells to evaluate the deviatoric term
2. Using one single subcell to calculate the volumetric term

This leads to the following elemental stiffness matrix

$$\tilde{K} = \mu \sum_{c=1}^{nc} \tilde{\boldsymbol{B}}_c^T \boldsymbol{D}_{dev} \tilde{\boldsymbol{B}}_c A_c + K \tilde{\boldsymbol{B}}^T \boldsymbol{D}_{\lambda} \tilde{\boldsymbol{B}} A^e d\Omega \tag{23}$$

where A_c is the area of the smoothing cell, Ω_C.

The resulting approach with selective smoothing cell brings out the stable and excellent convergence for compressible and nearly incompressible problems not only isotropic linear elasticity but also isotropic plasticity and viscoplasticity, etc.

4.NUMERICAL RESULTS

4.1. Cantilever beam

A 2-D cantilever beam subjected to parabolic loading at the free end is examined in this example as shown in Figure 3. The geometry is taken as length L, height D and thickness t, such that $L=8$, $D=4$ and $t=1$. The material properties are: Young's modulus $E=3x10^7$, and the amplitude of the parabolic shear force $P=250$. The exact solution of this problem is available as given by Reference [5]. Figure 4 illustrates a uniform mesh with 512 quadrilateral elements.

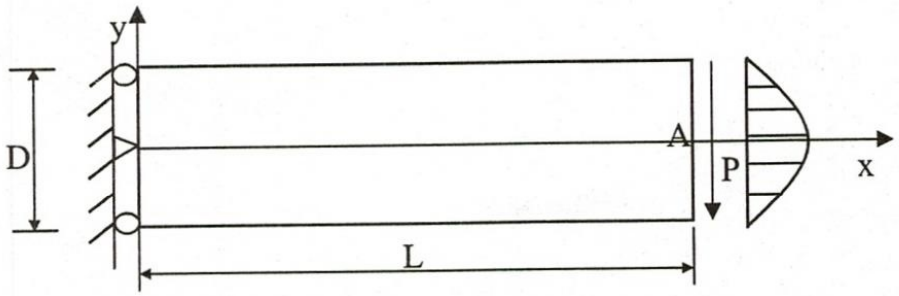

Figure 3. A cantilever beam and boundary conditions

The relative error in displacement norm is defined as

$$\mathrm{Re}_d = \sqrt{\sum_{i=1}^{ndof}\left(u_i^h - u_i^{exact}\right)^2 / \sum_{i=1}^{ndof}\left(u_i^{exact}\right)^2} \tag{24}$$

The error in energy is defined by

$$\left\|\boldsymbol{u}-\boldsymbol{u}^h\right\|_e = \left[\int_\Omega \left(\boldsymbol{\varepsilon}^h-\boldsymbol{\varepsilon}\right)^T \mathbf{D}\left(\boldsymbol{\varepsilon}^h-\boldsymbol{\varepsilon}\right)\right]^{1/2} \tag{25}$$

Under plane stress conditions, Poisson's ratio $\nu=0.3$, Figure 4 shows the relative error and the rate of convergence in the displacement norm for a sequence of uniform meshes, respectively.

From Figures 4 – 5, the presented method gives reliable results compared with 4-node FEM. Figures 4b and 5b show that the 2-Subcell, 3-Subcell and 4-Subcell elements exhibit the same convergence rate in both the L^2 and H^1 (energy) norms as the standard FEM. Moreover, displacement results for the 3-Subcell and 4-Subcell discretization are more accurate than the

standard bilinear Q4-FEM solution. The proposed elements also produce a better approximation of the strain energy. Additionally, the CPU time required for all elements presented here appears asymptotically lower than that of the FEM [6, 7], as the mesh size tends to zero.

Figure 5 shows the convergence in energy and the rate of the cantilever beam. Next we estimate the accuracy of the presented elements for the same beam problem, assuming a near incompressible material. Under plane strain condition, Figure 6 illustrates the displacements along the neutral axis for Poisson's ratio, $\nu = 0.4999$. The results show that FEM, 2–subcell, 3–subcell and 4–subcell solutions yield poor accuracy as Poisson's ratio ν tends toward 0.5. To remedy this locking phenomenon, selective integration techniques are considered. Figure 6b presents the results after of the selective integration method (SIM) to Q4-FEM element and using the selective cell-wise smoothing method for the FEM with strain smoothing [8].

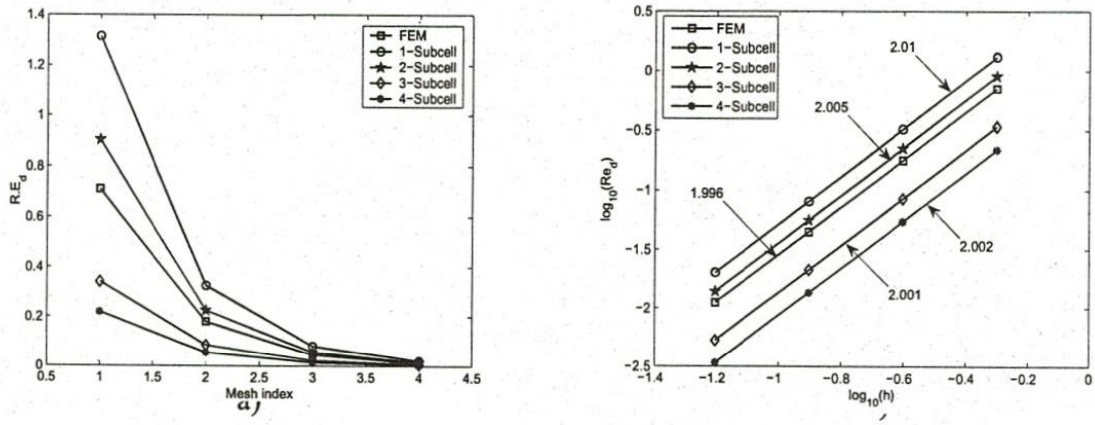

Figure 4: The convergence in displacement norm; a) the relative error, b) the rate

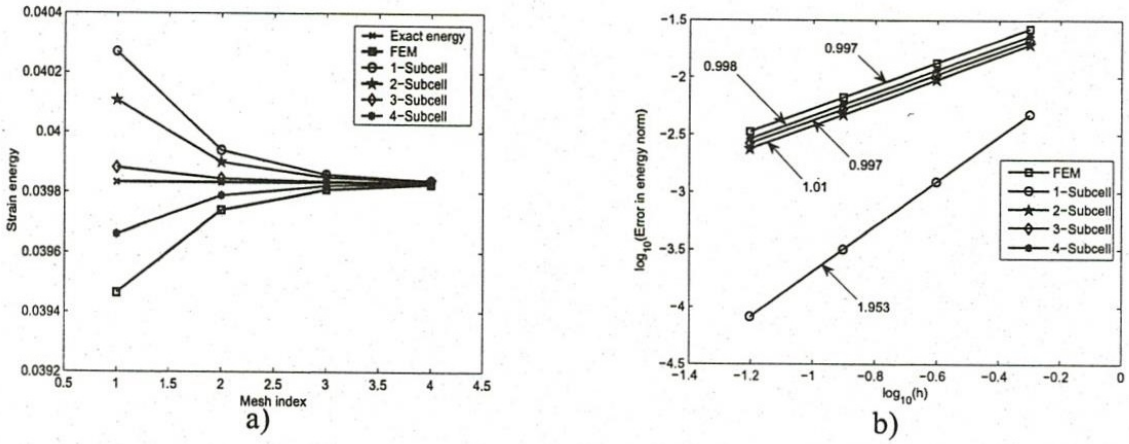

Figure 5. The convergence of the energy norm; a) the energy, b) the rate

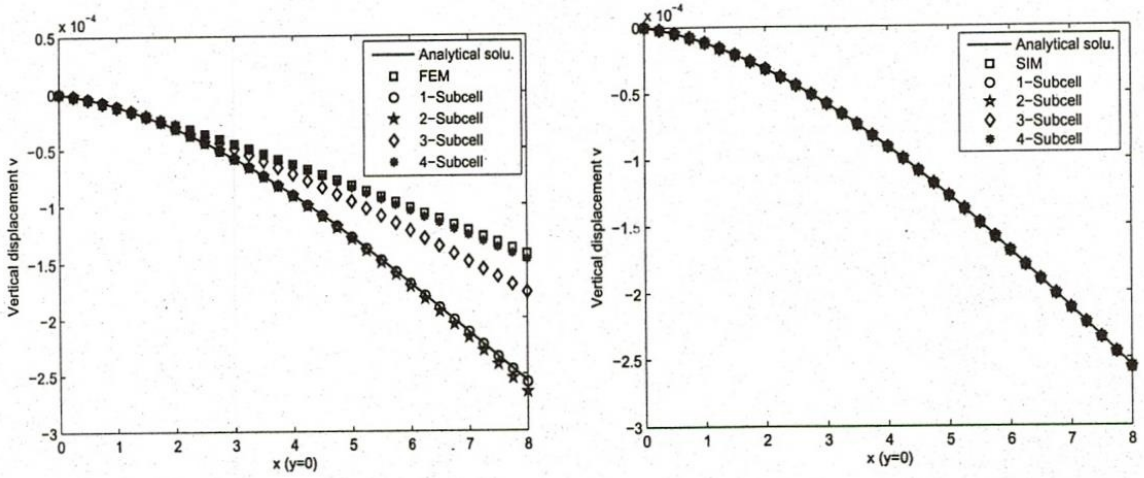

Figure 6: Vertical displacement for cantilever beam at the nodes along the x-axis (y =0): a) without using the selective technique, b) applying the selective method (ν = 0.4999)

4.2 L-shaped domain with applied tractions

Consider a L – shaped domain under plane stress condition applied tractions and boundary conditions are shown on Figure 7. The parameters of the structure are: $E = 1.0$, $\nu = 0.3$, $t = 1$. In this example, a stress singularity occurs at the re-entrant corner.

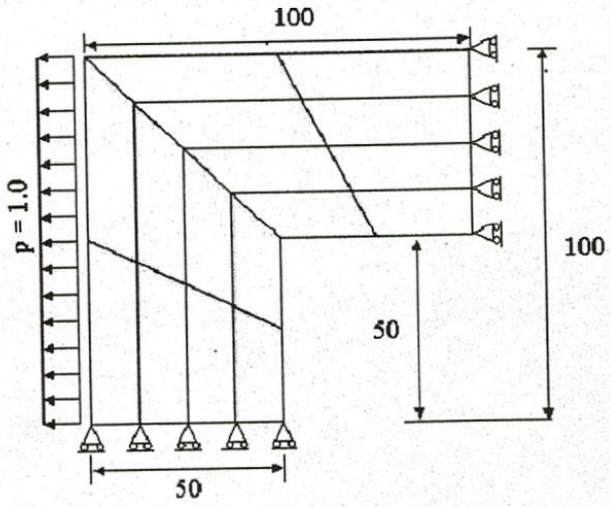

Figure 7: Domain problem and initial mesh

The convergence behaviour of overall strain energies is shown in Figure 8a, and the convergence rates are shown for comparison in Figure 8b with $\log_{10}(number\ of\ nodes)^{1/2}$. The accuracy of presented method is higher than that of the FEM-Q4. The 1-Subcell element provides the best solutions in strain energy for the coarser meshes. More particularly, an inversion of convergent energy for 2-Subcell and 3-Subcell is appeared. Two these Sub-cells lead to the less error than 4-Subcell and FEM do. Beside, a refined mesh towards to corner is necessary for purposing the reduction of error and computational cost.

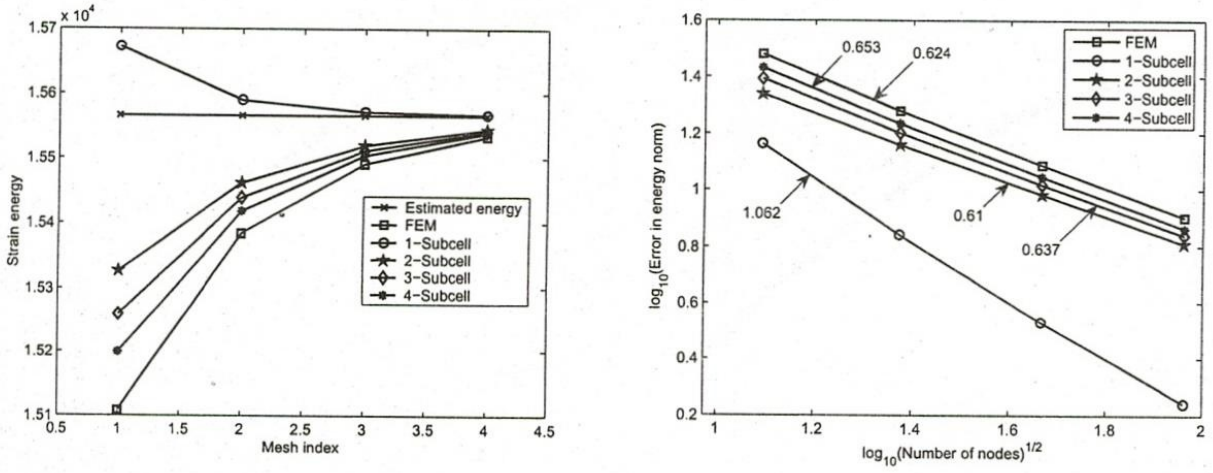

a) b)

Figure 8: The convergence of the energy norm; a) the strain energy, b) the rate

5. CONCLUSIONS

In this paper, we present a global aspect of the smoothed strains in finite element method to solve compressible and incompressible linear elastic. The element stiffness matrix is completely calculated along the boundary instead of the inside of element that the traditional FEM is utilized. The shape functions are calculated in a simple form. The numerical results show that the present method is normally more accurate than FEM while computational cost is not increasing.

The method is illustrated in two – dimensional linear elasticity but it can be extended to more complex structures such as non-linear elasticity, elastic – plastic behaviour and viscoplastics, plates, shell, 3D-problems, etc. The results of this investigation will be shown in forthcoming papers.

VỀ KỸ THUẬT TRƠN HÓA BIẾN DẠNG TRONG PHƯƠNG PHÁP PHẦN TỬ HỮU HẠN

Nguyễn Xuân Hùng[1] , Nguyễn Đình Hiển[2], Ngô Thành Phong[1]
(1)Trường Đại học Khoa học Tự nhiên, ĐHQG-HCM
(2)Trường Đại học Sư phạm Kỹ thuật Tp.HCM

TÓM TẮT: *Bài báo này trình bày một tổng quan về phương pháp trơn hoá biến dạng trong phần tử hữu hạn cho Cơ học vật rắn biến dạng hai chiều. Biến dạng tại mỗi điểm được chuẩn hóa bởi một hàm làm trơn trong một lân cận của miền khảo sát. Khi hàm trơn được chọn là hằng số, ma trận độ cứng được tính trên biên của phần tử thay vì bên trong như cách tính thông thường. Phương pháp đề cập đạt được độ chính xác cao hơn phương pháp phần tử hữu hạn truyền thống mà không tăng chi phí tính toán.*

REFERENCES

[1]. Chen JS, Wu CT, Yoon S, You Y. A stabilized conforming nodal integration for Galerkin mesh-free methods. *International Journal for Numerical Methods in Engineering,* 50:435 – 466 (2001).

[2]. Belytschko T, Lu YY, Gu L. Element – free Galerkin methods, *International Journal for Numerical Methods in Engineering,* 37:229 – 256 (1994).

[3]. Yoo JW, Moran B, Chen JS. Stabilized conforming nodal integration in the natural-element method. *International Journal for Numerical Methods in Engineering,* 60: 861 – 890 (2004).

[4]. Simo JC, Hughes TJR. On the variational foundation of assumed strain methods. *ASME Journal of Applied Mechanics,* 53:51 – 54 (1986).

[5]. Timoshenko S.P, Goodier J.N. Theory of Elasticity (*3rd edn).* New York, McGraw Hill, (1987).

[6]. G.R. Liu, K.Y. Dai, T.T Nguyen, A smoothed finite element for mechanics problems, *Computational Mechanics*, DOI 10.1007/s00466-006-0075-4, (2006).

[7]. Nguyen X.H, Bordas S, and Nguyen-Dang H, Finite element methods with stabilized conforming nodal integration: convergence, accuracy and properties, *International Journal Numerical Methods Engineering*, submitted (2006).

[8]. Nguyen X.H, Bordas S, Nguyen-Dang H. Smooth strain finite elements: selective integration, *Collection of papers from Prof. Nguyen-Dang Hung's former students*, Vietnam National University –HCM Publishing House, 88 -106 (2006).